 doi:10.20944/preprints202101.0594.v1

Article

New generation of hybrid materials based on gelatin and bio-active glass particles for bone tissue engineering

Amel Houaoui[1], Agata Szczodra[2], Mari Lallukka[2], Lamia El-Guermah[1], Remy Agniel[1], Emmanuel Pauthe[1], Jonathan Massera[2] and Michel Boissiere[1,*]

[1] Biomaterials for Health Research Group, ERRMECe, Equipe de recherche sur les Relations Matrice Extracellulaire-Cellules (EA1391), Institut des matériaux I-MAT (FD4122), CY Tech, CY Cergy Paris Université, Maison Internationale de la Recherche (MIR), rue Descartes, 95001 Neuville sur Oise cedex, France; amel.houaoui@cyu.fr (A.H.); lamia.el-guermah@cyu.fr (L.E); remy.agniel@cyu.fr (R.A); emmanuel.pauthe@cyu.fr (E.P.)

[2] Tampere University, Faculty of Medicine and Health Technology, Laboratory of Biomaterials and Tissue Engineering, Korkeakoulunkatu 3, 33720, Tampere, Finland; agata.szczodra@tuni.fi (A.S.); mari.lallukka@polito.it (M.L.); jonathan.massera@tuni.fr (J.M.)

* Correspondence: michel.boissiere@cyu.fr (M.B.); Tel +33-01-34-25-75-61

Abstract: Hybrid scaffolds based on bioactive glass (BAG) particles (<38µm), covalently linked to the gelatin (G*), using 3-glycidoxypropyltrimethoxysilane (GPTMS), have been studied for bone bioengineering. In this study, two glass compositions (13-93 and 13-93B20 [where 20% of the SiO_2 was replaced with B_2O_3]) were introduced in the gelatin matrix. The C_{factor} (Gelatin/GPTMS molar ratio) was kept constant at 500. The hybrids obtained were found to be stable at 37°C, in solution; condition at which pure gelatin is liquid. All hybrids were characterized by in vitro dissolution in TRIS solution (for up to 4 weeks) and Simulated Body Fluid (SBF) (for up to 2 weeks). Samples processed with 13-93B20 exhibit a faster initial dissolution and significantly faster precipitation of a hydroxyapatite (HA) layer. The faster ion release and HA precipitation recorded from the G*/13-93B20 samples, is attributable to the higher reactivity of borosilicate compared to the silicate glass. MC3T3-E1 cells behavior, in direct contact with the hybrids, was investigated, showing that the cells were able to proliferate and spread on the developed biomaterials. Tailoring the glass composition allows to better control the material's dissolution, biodegradability, and bioactivity. Bioactive (especially with 13-93B20 BAG), and biocompatible, the hybrids are promising for bone application.

Citation: Lastname, F.; Lastname, F.; Lastname, F. Title. *Biomolecules* **2021**, *11*, x. https://doi.org/10.3390/xxxxx

Keywords: Hybrid scaffold; Bioactive Glass; Gelatin; GPTMS; Bone tissue engineering

1. Introduction

Bone fractures are a common trauma. For a large loss of bone substance (defect greater than 1 cm^3) following a traumatic situation, as a pathology or accidental defect, the natural process of self-repair is compromised [1]. Tissue engineering is an innovative approach used for bone repair. Bone reconstruction is assisted with materials which will participate in tissue regeneration [2,3]. These materials must have the properties adapted to this function.

Bioactive ceramics are of interest in bone regeneration. The bioactivity of these materials results in the appearance of biological activity in the host organism and the existence of ion exchanges between the material and living tissue [4]. Synthetic hydroxyapatite (HA) and β-tricalcium phosphate (β-TCP) are the more widely used [5–7]. They often have osteoconductive and sometimes osteoinductive properties. However, their crystalline structure differs from that of the mineral phase of natural bone, which causes a slow resorption, and thus limits their clinical relevance [8,9]. Indeed, the limited resorption of those ceramics was demonstrated, in-vivo, when used in cements [10].

 doi:10.20944/preprints202101.0594.v1

Bioactive Glass (BAG) is a sub-category of ceramics, and are osteoconductive, but also osteoinductive [11]. These glasses are mainly used for hard tissue reconstruction, but they are also able to bond to soft tissue [12]. However, due to their brittleness, shaping the glass into its final shape remains a challenge. Organic/inorganic composite scaffolds represent a convenient alternative to traditional BAG. They allow the possibility to tailor the mechanical properties, degradation kinetics and bioactivity. Current research is focused on the fabrication of bioactive composite materials, with the bioactive phase incorporated as filler into the bioresorbable polymer matrix [13]. However, a drawback with many conventional composites is that the constituent phases interact on a micrometer scale, which can result in differential resorption rates during dissolution and masking of the bioactive component. This would inevitably lead to material instability in vivo [14].

Hybrid scaffolds are materials where the organic and inorganic phase interact chemically on a nanoscale allowing to control the properties of the final material, for instance degradation rates and mechanical properties [14–16]. Moreover, the inorganic and organic content in addition to the degree of covalent links can be adjusted to have a precise control of the hybrid properties as stiffness and dissolution rates leading to a material adapted for a specific application [14]. For the hybrids' formation, covalent links between the organic and inorganic matrix are fundamental. They can be obtained through reaction with organosilanes such as 3-glycidoxypropyltrimethoxysilane (GPTMS) or 3-aminopropyltriethoxysilane (APTES) [17–20].

In our work, we present hybrid materials for bone tissue engineering based on gelatin and BAG (Figure 1), where two BAGs, with different composition (13-93 and 13-93B20), are compared. 13-93 is a FDA approved BAG that exhibits slower dissolution rate than the commercialized BAGs 45S5 or S53P4 [21,22]. The rational for studying 13-93 BAG lies in preventing an excessive dissolution of the glass particles during processing, degradation of the organic phase, a decrease of the mechanical properties and a fast release of ions which could be toxic for the cells. 13-93B20, a similar composition than 13-93 but with 20% of the SiO_2 substituted with B_2O_3, was also included in the study. It has been showed that the borosilicate glasses based on the 13-93 composition have faster in-vitro dissolution but also faster conversion into HA, while maintaining a slower dissolution kinetics than 45S5 and S53P4 [13,23,24].

Here, two hybrid materials were studied, based on gelatin and 13-93 or 13-93B20. The content of organic and inorganic matrix was 70/30 (wt%) respectively and a C_{factor} (degree of covalent coupling, molar ratio of GPTMS/gelatin) of 500 was used. To investigate their in-vitro dissolution behavior, the hybrids were immersed in TRIS buffer solution for one month. Ion release from the glass was quantified and the mineral content was measured. The compressive properties of the hybrids were studied during the immersion. The bioactivity, assumed to be related to the precipitation of a HA layer at the materials' surface when immersed in aqueous solution, was assessed in Simulated Body Fluid (SBF) [25]. Preliminary cell experiments were performed to assess cell activity by culturing MC3T3-E1 pre-osteoblastic cells at the surface of the hybrids. Cell proliferation and morphology were studied. The aim of this study was to assess the behavior of the hybrids, in vitro, in aqueous solutions and its biocompatibility.

Preprints (www.preprints.org) | NOT PEER-REVIEWED | Posted: 28 January 2021 doi:10.20944/preprints202101.0594.v1

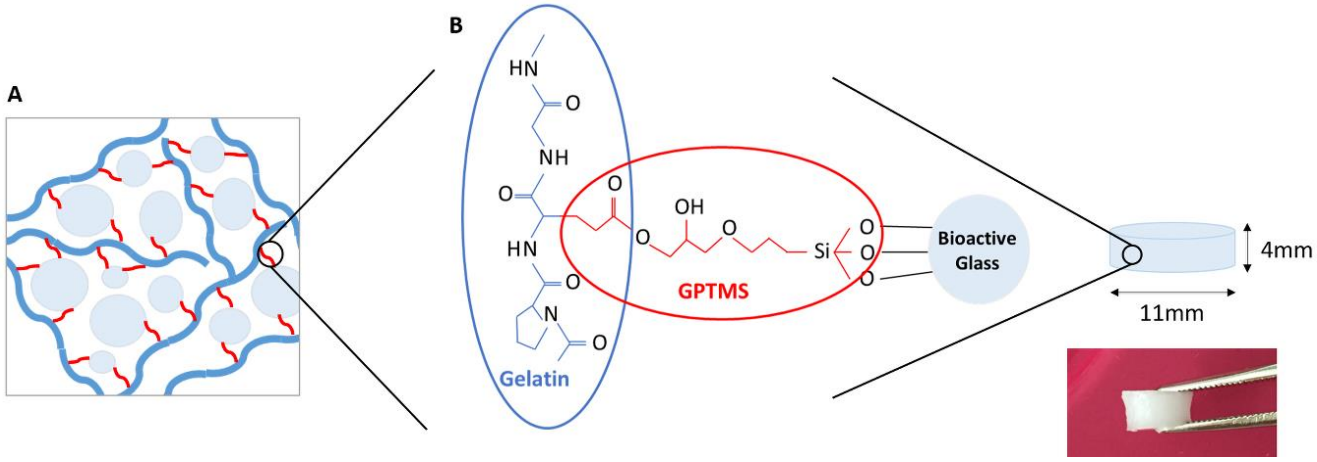

Figure 1: A) Schematic representation (inspired from Mahony et Al. [18]) and B) chemical structure of the hybrid made of gelatin and BAG covalently linked by the GPTMS.

2. Materials and Methods

2.1 Materials preparation and characterization

2.1.1 Bioactive glass processing

BAG 13-93 and 13-93B20 were prepared from analytical grade K_2CO_3 (Alfa Aesar, Haverhill, USA), (Na_2CO_3, $NH_4H_2PO_4$, ($CaHPO_4$)(2($H2O$)), $CaCO_3$, MgO, H_3BO_3 (Sigma Aldrich, Saint-Louis, MS, USA) and Belgian quartz sand. The 100-gram batches of 13-93 and 13-93B20 were melted for 3 hours at 1450°C, in a platinum crucible. The molten glasses were cast, annealed, crushed, and finally sieved into less than 38µm particles. The glasses were dried at 200°C for 2 hours prior to be used. The nominal oxide compositions of the glasses are given in Table 1.

Table 1: Nominal glass composition (%)

Glass	mol%						
	Na_2O	K_2O	MgO	CaO	P_2O_5	SiO_2	B_2O_3
13-93	6.0	7.9	7.7	22.1	1.7	54.6	-
13-93B20	6.0	7.9	7.7	22.1	1.7	43.7	10.9

2.1.2 Hybrids synthesis

Gelatin (Porcine, Type A, Bloom 300, Sigma Aldrich) was dissolved at 37°C in 10 mM hydrochloric acid (HCl) at a concentration of 50 mg.mL−1. This solution was functionalized by adding the appropriate amount of GPTMS (Sigma Aldrich) to have a Cfactor (molar ratio of GPTMS/gelatin) of 500. The functionalized gelatin (G*) solution was left to mix 2h at 37°C. Then the appropriate amount of 13-93 or 13-93B20 was added in the solution to have a content of G*/BAG of 70/30 wt%. The solution was mixed for 1h at 37°C. Once the G* solution (sol) has mixed with the BAG, sodium fluoride (NaF, 1%, Sigma Aldrich) was added to the sol at sol/NaF volume ratio of 100/10 to catalyze the inorganic condensation reaction. The final solution was mixed 10min at 37°C, then poured in silicon molds and let to gel at room temperature for 24h.

Hybrid materials with a diameter of 11mm and height of 4mm were cut. To measure their glass content, they were freeze-dried and heated 2h at 500°C under air to remove all

Preprints (www.preprints.org) | NOT PEER-REVIEWED | Posted: 28 January 2021 doi:10.20944/preprints202101.0594.v1

the organic phase. The remaining mineral phase was weighed. The measure was repeated on 4 samples per composition and the average glass content with standard deviation calculated.

2.2 Behavior of G/BAG hybrids*

2.2.1 Physico-chemical properties of the hybrids

- Immersion in TRIS

Tris(hydroxymethyl)aminomethane (TRIS) solution (50mM) was prepared by mixing ultra-pure TRIS and TRIS-HCl (Sigma Aldrich) in ultra-pure water and the pH was adjusted to 7.4 at 37°C. The samples were cut to obtain small cylinder of 11mm of diameter and 4mm of height (≃380 mg) which were immersed in 30mL of TRIS solution for up to 28 days at 37°C on an agitator (Heidolph Instruments) with an orbital speed of 100rpm. To avoid saturation of the solution with the ions released from the hybrids, TRIS buffer was refreshed each week.

At desired time of immersion, the concentration of elements released from the hybrids was studied by diluting 500µL of the immersion solution in 4.5 mL of ultra-pure water for ion analysis. ICP-OES (Agilent technologies 5110) was employed to quantify P (λ = 253.561 nm), Ca (λ = 422.673 nm), Mg (λ = 279.553 nm), Si (λ = 250.690 nm), B (λ = 249.678 nm), K (λ = 766.491 nm) and Na (λ = 589.592 nm) concentrations in the solution after samples immersion. The measurements were conducted in four separate samples at each time points for each composition and the results are presented as mean ± standard deviation (SD).

- Mineral content in hybrids

Mineral mass after the samples' synthesis and at various immersion times was measured after freeze-drying and burning the samples 2h at 500°C, under air, to remove all the organic phase. The remaining mineral phase was weighed. The measurements were conducted on four separate samples at each time points for each composition and the results are presented as mean ± SD.

- Mechanical properties of the hybrids

Mechanical properties of the hybrids after synthesis and after immersion (wet) were tested by compression test at room temperature using a texturometer (LS1, Lloyd Instruments, Ametek). The measurements were conducted on four separate samples at each time points for each composition. A 20 N load cell was used for testing, with a compression extension speed of 1 mm.min-1. The results are presented as mean ± SD.

2.2.2 Hybrids bioactivity

- Immersion in Simulated Body Fluid (SBF)

Developed by Kokubo et al., SBF was prepared following the methodology from the standard ISO/FDIS 23317 [27]. The samples were cut to obtain small cylinder of 11mm of diameter and 4mm of height (≃380 mg) which were immersed in 30mL of SBF for up to 2 weeks at 37°C in a shaking incubator (Heidolph Instruments) with an orbital speed of 100rpm. During the experiment, the solution was not refreshed to study the precipitation of calcium-phosphate. The ion concentration in the solution according to immersion time was measured as previously described. The measurements were conducted in four separate samples at each time points for each composition and the results are presented as mean ± SD.

- Mineral content in hybrids

Preprints (www.preprints.org) | NOT PEER-REVIEWED | Posted: 28 January 2021 doi:10.20944/preprints202101.0594.v1

Mineral mass after various immersion times was measured as explained above. Measurements were conducted on four separate samples at each time points for each composition and the results are presented as mean ± SD.

- Hybrids surface analysis

The reactive layer at the hybrids surface after immersion in SBF was observed by SEM (GEMINISEM 300 from Zeiss) and its composition was analyzed by Energy-Dispersive X-ray spectroscopy (EDX Quantax from BRUKER). The Infrared (IR) absorption spectra of the hybrids immersed in SBF were also recorded using a Bruker Alpha FTIR in Attenuated Total Reflectance (ATR) mode. The measurements were performed on dry samples. All IR spectra were recorded within the range 399–4000 cm-1 with a resolution of 2 cm-1 and 32 accumulation scans.

2.2.3 Cell analysis

- Hybrids preparation

G*/13-93 and G*/13-93B20 hybrids were synthesized in sterile conditions. The samples were cut to obtain small cylinders of 11mm of diameter and 4mm of height. Each material of each condition was immersed in sterile TRIS solution during 10 days at 37°C to remove excess components. After that, all cell experiments were performed in 48-well plates.

- Cell culture

Pre-osteoblastic MC3T3-E1 cells were cultured in α-MEM containing glutamine supplemented with 10 % Fetal Bovine Serum (FBS), 1 % penicillin/streptomycin. The cells were cultured with a humidified atmosphere of 5 % CO_2 at 37 °C.

- Cell proliferation

To compare the behavior of MC3T3-E1 cells on the different samples, cell proliferation was studied using CyQUANT Cell Proliferation Assay kit (Invitrogen, Life Technologies). The control used was the Tissue Culture Polystyrene (TCPS) 48 well-plate. The hybrids were placed in the wells and 5000 cells/well were seeded and the medium was changed every 2 days. After 1, 3, 7, 10 and 14 days of culture, the cells were lysed with 700 µL 0.1 % Triton-X100 (Sigma–Aldrich) buffer and conserved at -80 °C. After one freeze–thaw-cycle, three 20 µl aliquots of each lysate were pipetted to a black 96-well plate (Corning) and mixed with 180 µl working solution containing CyQUANT GR dye and cell lysis buffer. The fluorescence at 520nm was measured with a Spectrofluorimeter Xenius XM (SAFAS).

- Cell morphology

The morphology of the cells on the different samples was observed after 1, 7 and 14 days of culture. The control used was TCPS coverslips of 13mm diameter in 24-well plate. The number of cells was adjusted according to the well area. The same density of cells was seeded on the hybrids and the TCPS coverslips controls and after each time point, the cells were fixed with 4 % (w/v) para-formaldehyde solution for 15 min, then permeabilized with 0.1 % (v/v) Triton X-100 (Sigma Aldrich) for 10 min. Non-specific binding sites were blocked by incubating the disks in PBS containing 1 % Bovine Serum Albumin (BSA) for 1 h. The cytoskeleton and nuclei of the cells were stained respectively with 1:500 diluted TRITC-labelled phalloidin (Sigma Aldrich P5282) and 1:1000 diluted 4',6-Diamidino-2-phenylindole dihydrochloride (DAPI, Sigma Aldrich D9542) in PBS-BSA 0.5 % for 1 h. Each incubation with antibodies was performed in wet and dark. Samples were then washed in PBS-BSA 0.5 % and pure water and observed using a LSM710 confocal microscope (Carl Zeiss).

- Statistical analysis

Preprints (www.preprints.org) | NOT PEER-REVIEWED | Posted: 28 January 2021 doi:10.20944/preprints202101.0594.v1

Data are analyzed using GraphPad Prism Software. Statistical significance between groups is assessed by one-way analysis of variance (ANOVA). Experimental results are expressed as means ± standard deviation. Statistical significance is taken for values of $p < 0.01$.

3. Results and discussion

The aim of this study is to develop hybrid materials based on gelatin and BAG able to release therapeutic ions for bone regeneration while controlling the dissolution properties of the organic and inorganic phases of the scaffold. The first step was to determine the optimal C_{factor} for the targeted applications. Indeed, the higher is the C_{factor}, the more covalent links will be formed in the structure. However, an excess of GPTMS can lead to excessive unreacted precursor, leading to a cellular toxicity [14,26]. Thus, to avoid this negative effect, studies have led us to use a C_{factor} of 500 for our hybrids (data not shown). Thereby, the BAG 13-93 and 13-93B20 were covalently linked to the gelatin with a C_{factor} of 500. The materials dissolution in aqueous solutions and their bioactivity were compared.

3.1 Characterization of the hybrids after synthesis

Table 2 presents the glass loading in the hybrids and their young modulus after synthesis. The mineral mass in the hybrids was determined after freeze-drying and burning the inorganic phase at 500°C under air for 2h. Table 2 shows that the glass loading is 34±2 wt% and 33±1 wt% for the G*/13-93 and G*/13-93B20 respectively, as expected from the targeted loading.

Table 2: Measured glass loading and Young modulus of the gelatin alone functionalized (G*) and the G*/13-93 and G*/13-93B20 hybrids (for wet samples, the mechanical properties were measured after 10min of immersion in TRIS).

Materials	Glass loading in the hybrids (wt%)	Young modulus (GPa)	
		Dry samples	Wet samples
G* alone	--	2.1 ± 0.3	0.8 ± 0.2
G*/13-93	34 ± 2	0.5 ± 0.3	0.5 ± 0.1
G*/13-93B20	33 ± 1	0.7 ± 0.2	0.6 ± 0.2

The Young modulus of G* alone and the hybrids were measured by a compression test. Both hybrids have young modulus stable in wet and dry conditions. The Young modulus of the hybrids compared to G* alone is lower. This decrease of Young modulus appears when the BAG is added to the G*. That shows that adding the glass in the organic phase influences the mechanical properties of the scaffold. This decrease happens with both BAG, showing that the type of glass does not have any effect on the scaffold mechanical properties. These lower mechanical properties when adding the inorganic phase are probably due to the glass which induces defects on the structure, leading to a modification of the organic network.

3.2 Behavior of the hybrids in solution

Resorbable materials needs to present controlled degradation and sufficient mechanical properties until the bone tissue regeneration [27]. Their bioactivity is a fundamental property which will help bone repair. To assess these properties the hybrids were immersed in aqueous solutions and their dissolution was studied.

3.2.1 Dissolution in TRIS

Preprints (www.preprints.org) | NOT PEER-REVIEWED | Posted: 28 January 2021 doi:10.20944/preprints202101.0594.v1

The hybrids degradation in TRIS was studied by mass measurements, ICP-OES analysis and compression tests. These tests could not be done on the G* without BAG because it was dissolving at 37°C, contrary to the G*/13-93 or 13-93B20. This shows that the materials made of gelatin and BAG, covalently linked by the GPTMS, can be considered as hybrids. Moreover, Mahony et Al. worked on hybrids based on gelatin and silica network coming from TEOS hydrolysis and condensation and showed that the GPTMS is efficient in creating covalent links between both matrices [14]. Figure 2 presents the mass loss of the hybrids as a function of the immersion time (Figure 2A), the hybrid mass after freeze-drying (Figure 2B), and the mineral mass remaining in the materials after immersion (Figure 2C).

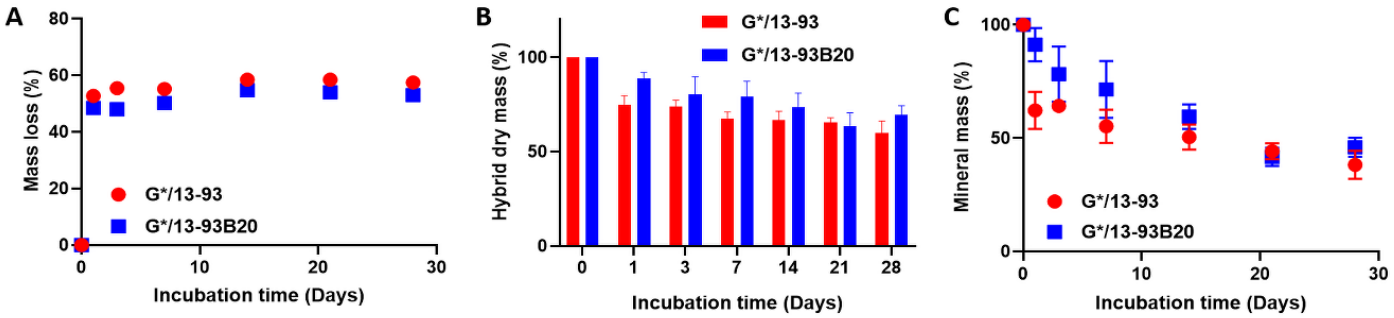

Figure 2: Mass loss (A), dry mass (B) and mineral mass (C) remained in the hybrid G*/13-93 (●) and G*/13-93B20 (■) as a function of immersion time in TRIS.

Mass loss graph (Figure 2A) shows that after 24h, the mass loss reaches 50% and remained stable at longer immersion time. The same results are observed for the G*/13-93 and the G*/13-93B20 showing that this mass loss is not dependent of the type of the glass. On Figure 2B, a decrease of the hybrids dry mass is observable. At 24h, the hybrids dry mass goes from 100% to 75% and 89% for the G*/13-93 and the G/*13-93B20 respectively and does not reach 50% during the immersion. This result does not corroborate the mass loss at 24h on Figure 2A. This would mean that during the first 24h, the hybrids loose mostly water. This can be seen from a macroscopic point of view on the hybrids which shrink and loose 2mm of diameter and 1mm of height after 24h of immersion, indicating a rearrangement of the hybrids structure, due to a syneresis phenomenon.

On the Figure 2B, the hybrids dry mass decreases with immersion time exhibiting a dissolution of the material. On Figure 2C, the mineral mass decreases with immersion time. This result shows that the 13-93 and the 13-93B20 are dissolving in TRIS solution during the immersion. This is further confirmed by the quantification of the ion release in solution (Figure 3).

For both hybrids, all ions from the BAG are found to leach out into the solution showing that the glasses are dissolving through the gelatin. The Si release from the G*/13-93B20 is continuously increasing and slightly lower than for G*/13-93. Moreover, the initial release of Mg, Na, K, and Ca elements is faster for the G*/13-93B20 than for G*/13-93. This can be due to the fact that the borosilicate glass would be more reactive with the siloxane than G*/13-93, leading to a lower Si release from the hybrids with 13-93B20 than the one with 13-93. The release of the elements coming from the G*/13-93B20 directly reaches the plateau from the beginning of the immersion while it increases for the G*/13-93 until reaching the same plateau (Figure 3 and 4). For the G*/13-93 (Figure 4A), it appears that the glass dissolution is limited for the Ca, K, Mg, with a plateau reached at 14 days and approximately 20% of these elements released in solution. The Si and Na releases seem to be higher than the first ions cited, linear and continuous for 28 days. Figure 4B) presents the release of ions from the hybrids containing the 13-93B20 glass. For the Ca, K, Mg and B, the release of these elements is already at the plateau from the first time point contrary

Preprints (www.preprints.org) | NOT PEER-REVIEWED | Posted: 28 January 2021 doi:10.20944/preprints202101.0594.v1

to the hybrid containing 13-93 (results also observed in Figure 3). This plateau, reached from the beginning of the immersion at 20% (as for the G*/13-93), shows also that the initial dissolution of the G*/13-93B20 is faster than for G*/13-93.

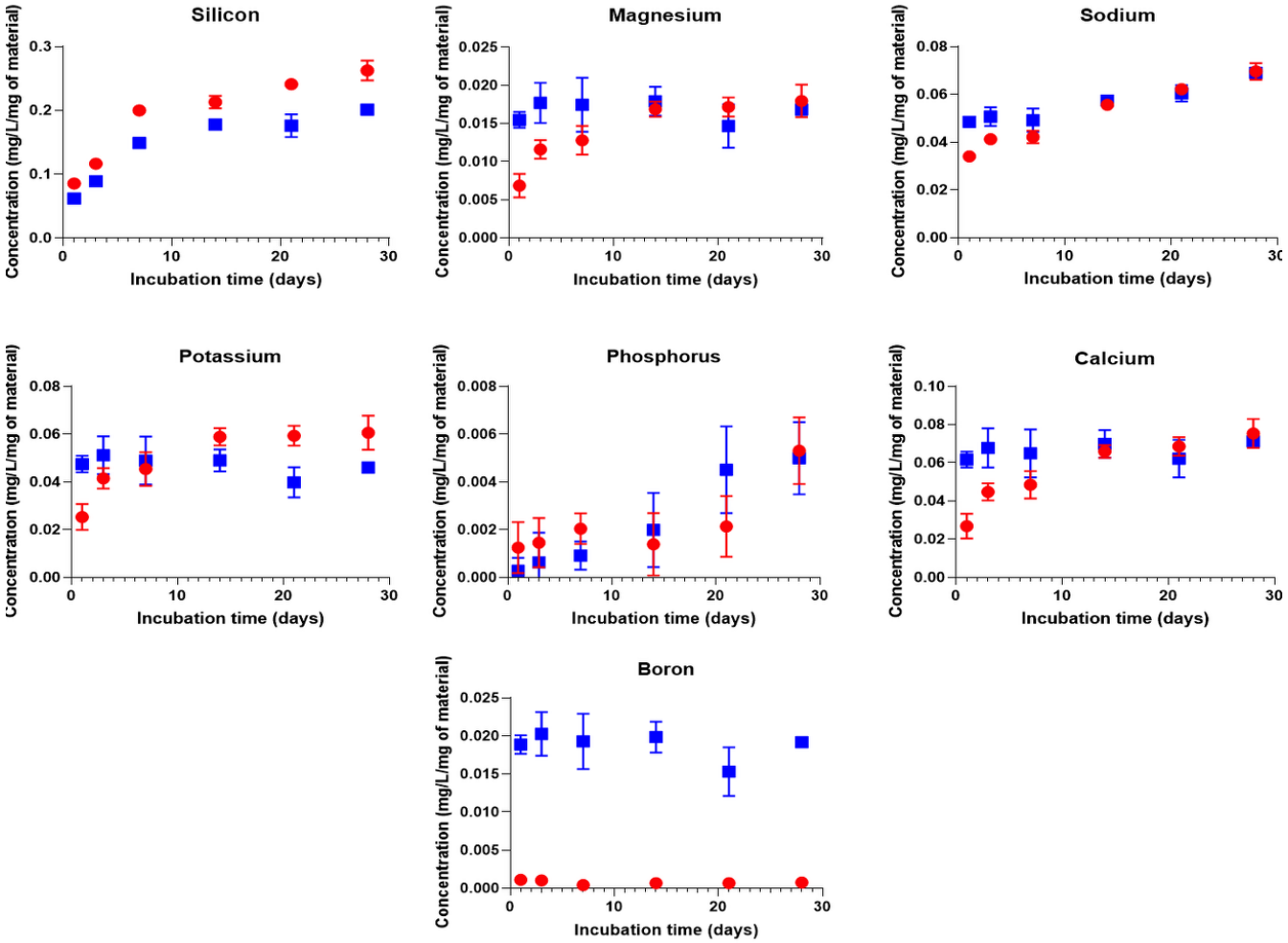

Figure 3: Elements concentrations of Si, Mg, Na, K, P, Ca, and B in the dissolution products of G*/13-93 (●) and G*/13-93B20 (■) immersed in TRIS as a function of time. The concentrations are normalized to the sample mass.

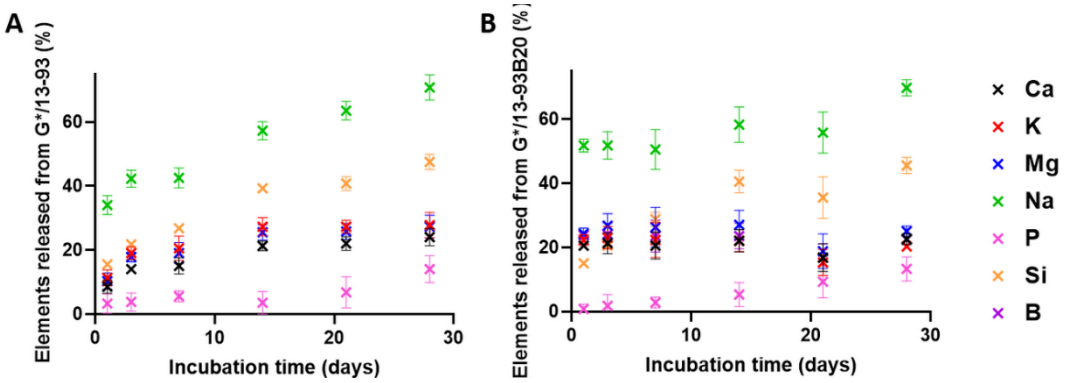

Figure 4: Release of ions from the A) G*/13-93 and B) G*/13-93B20 hybrids, immersed in TRIS as a function of time.

Preprints (www.preprints.org) | NOT PEER-REVIEWED | Posted: 28 January 2021 doi:10.20944/preprints202101.0594.v1

For both hybrids, the Si and Na releases are more important than for the other elements, with a Na release already stable from the first time point for G*/13-93B20. The higher concentrations of Si and Na are probably because they come from the glass but also from the GPTMS and NaF respectively. The important release of Si in solution is probably followed by a condensation and polymerization, forming an amorphous silica-rich layer around the glass [28], slowing down the release of the Ca, Mg, K and B (for G*/13-93).

After analyzing the degradation of the hybrids, their mechanical properties were studied by doing a compression test on wet samples during the immersion (Figure 5).

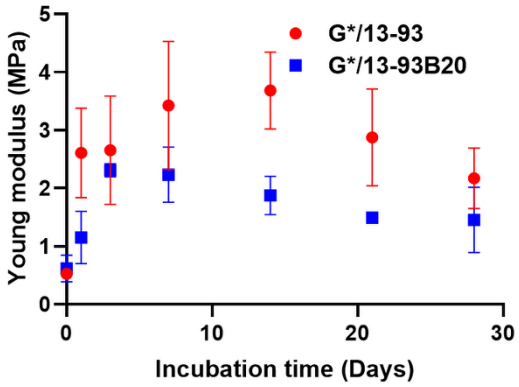

Figure 5: Young modulus measured by a compression test of wet G*/13-93 (●) and G*/13-93B20 (■) hybrids as a function of immersion time in TRIS.

The Young modulus was measured on wet samples as a function of incubation time (Figure 5). The evolution of the mechanical properties takes place in two stages. First an increase of the Young modulus for both hybrids can be seen. A maximum is then reached at 3 days for G*/13-93B20 and 14 days for G*/13-93. At longer immersion time, a decrease of the Young modulus is noticed. The increase of the modulus could be due to the syneresis phenomenon as explained for Figure 2. The water loss would lead to a reinforcement of the mechanical properties. After that, the decrease of the Young modulus would be due to hybrids erosion, inducing a loss of its mechanical properties. This corroborates the phenomenon showed in Figure 3 and 4, showing that this decrease happens when the stabilization of ions release is reached for G*/13-93.

Hybrids immersion in TRIS allowed to understand their dissolution and their ions release in solution. The 13-93B20 dissolves and reaches the saturation faster but finally at the same level than the 13-93. This dissolution has an influence on the mechanical properties but it should be noted that despite these variations, the Young modulus stays close to that of cancellous bone [29].

3.2.2 Dissolution in Simulated Body Fluid (SBF)

The hybrids were immersed in Simulated Body Fluid (SBF) to study their bioactivity. ICP-OES analysis, mass measurements, SEM observations, and EDX and FTIR analysis were conducted to assess the ion release/precipitation and the formation of a reactive layer.

As postulated by L.L. Hench, the ability of a material to induce the precipitation of an hydroxyapatite layer at its surface can be considered as a sign of bioactivity [11]. Immersion in SBF was conducted for two weeks and the solution was not refreshed. The ions concentration in the solution was quantified. The difference between the ions' concentration in SBF and ions concentration after hybrid immersion was calculated (Figure 6).

The Ca concentration seems to increase initially and then decreases with immersion time, whereas the P concentration decreases from the beginning of the dissolution. This

Preprints (www.preprints.org) | NOT PEER-REVIEWED | Posted: 28 January 2021 doi:10.20944/preprints202101.0594.v1

phenomenon was also observed in our previous study on composites based on PLA and the same glasses [13]. Generally, the decrease in Ca and P in SBF would correspond to the precipitation of a calcium-phosphate reactive layer. The elements Mg and K show similar trends during immersion in SBF. The 13-93B20 glass leaches out its ions at faster rate initially than 13-93 and then; for both hybrids, a decrease of Mg and K concentrations appears. It is important to note that the dissolution rate slows down at earlier immersion time in SBF than in TRIS for G*/13-93. This decrease shows the saturation of the solution and probably that Mg and K can be incorporated into the calcium-phosphate reactive layer [30]. Silicon release is linear and continuous, tending towards a plateau, for both hybrids. It is initially higher for G*/13-93, which can be, as explained above, because the borosilicate glass would be more reactive with the siloxane leading to a lower Si release from the hybrids with 13-93B20.

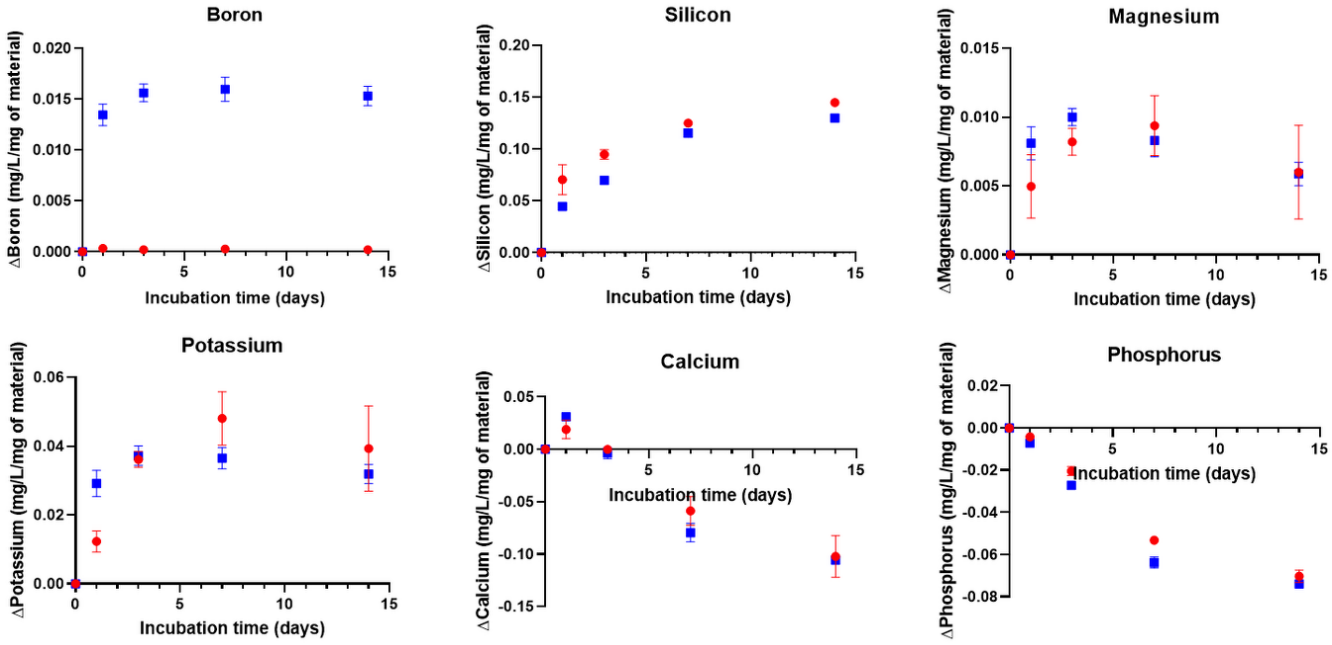

Figure 6: Elements concentrations of Si, Mg, K, P, Ca and B in the dissolution products of G*/13-93 (●) and G*/13-93B20 (■) immersed in SBF as a function of time. The concentrations are normalized to the sample mass. ΔElement = [Element] in SBF in presence of the sample – [Element] in SBF initial solution.

Figure 7 presents the mass loss of the hybrids as a function to immersion time in SBF (Figure 7A), the hybrid mass after freeze-drying (Figure 7B), and the mineral mass remaining in the materials after immersion (Figure 7C).

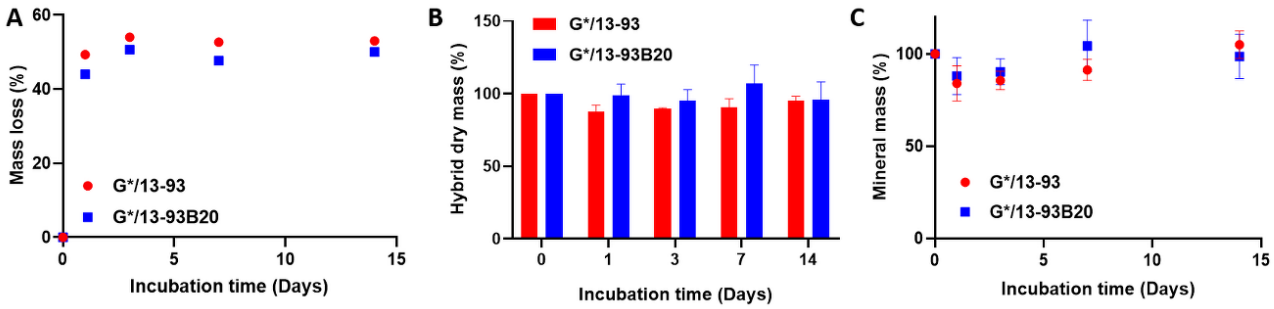

Figure 7: Mass loss (A), dry mass (B) and mineral mass (C) remained in the hybrid G*/13-93 (●) and G*/13-93B20 (■) as a function of immersion time in SBF.

Preprints (www.preprints.org) | NOT PEER-REVIEWED | Posted: 28 January 2021 doi:10.20944/preprints202101.0594.v1

Figure 7A shows that after 24h, the mass loss reaches approximately 50% corresponding to a water loss and thus a shrinking of the materials due to the syneresis as explained for TRIS immersion. Then, the mass loss stays stable during immersion. On Figure 7B, the dry mass of hybrids immersed in SBF does not show same evolution as in TRIS immersion. Indeed, a decrease of the dry mass was observed in TRIS immersion, while in SBF it appears to stay approximately stable. For the mineral mass (Figure 7C), while it was decreasing during immersion in TRIS showing the dissolution of the glasses, in SBF, it is decreasing and then increasing. This would correspond to the dissolution of the glass, followed by the precipitation of the calcium-phosphate layer.

To assess the precipitation of this reactive layer, the hybrids were observed and analyzed using SEM/EDX as well as FTIR (Figure 8 and 9).

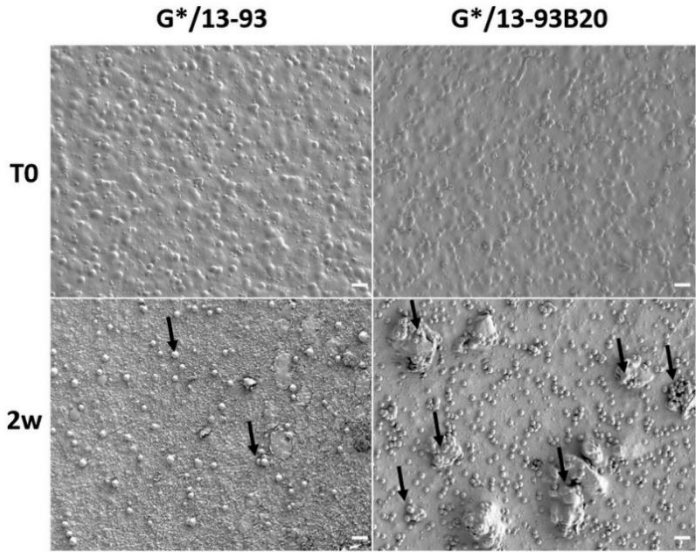

Figure 8: SEM image of the hybrids surface before and after 14 days of immersion in SBF (scale bar 20µm).

After 2 weeks of immersion in SBF, nodules appear at their surface. The nodules are small and dispersed on the hybrid containing 13-93 while they are more numerous and larger at the G*/13-93B20 hybrid surface. EDX analysis were performed on the nodules shown in Figure 8 and the spectra are presented in Figure 9A. The composition of the spheres from both hybrids is mainly Ca and P with a ratio of Ca/P of 1.77 ± 0.08 which is close to hydroxyapatite [31]. This corroborates the precipitation of calcium-phosphate layer hypothesized from the ICP analysis (Figure 6). It is interesting to point out that the materials containing the glass 13-93B20 exhibit a higher population and bigger nodules than materials processed with the glass 13-93. This is in agreement with Huang et al. who demonstrated that the borosilicate bioactive glasses, convert into HA faster and more completely than their silicate counterpart [32].

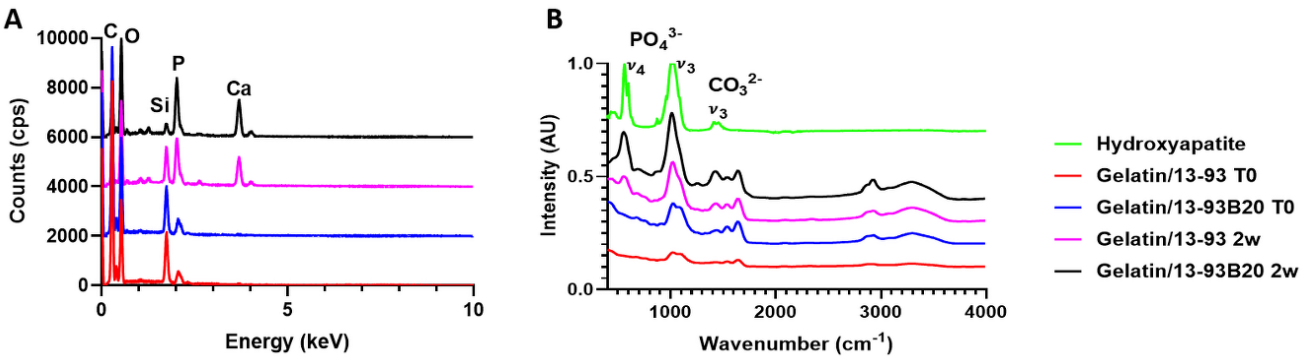

Preprints (www.preprints.org) | NOT PEER-REVIEWED | Posted: 28 January 2021 doi:10.20944/preprints202101.0594.v1

Figure 9: A) EDX analysis of the nodules at the hybrids surface and B) FTIR analysis of the samples surfaces before and after 14 days of immersion.

The nature of the Ca/P precipitate was further analyzed by FTIR spectroscopy (Figure 9B). Two peaks in the 500-600 cm-1 and ≈1000 cm-1 appear after G*/13-93B20 (they are also present for G*/13-93 but with a lower intensity) immersion in SBF. These peaks correspond to the ν_4 (P – O bending) and ν_3 (P – O stretching) PO_4^{3-} vibrations respectively in apatite structure. The carbonate CO_3^{2-} vibration is also present [33–35]. These peaks are characteristic of a hydroxyapatite structure. This is a good indication that the calcium phosphate layer precipitating on the hybrids surface is a hydroxy-carbonated apatite, indicative of the potential bioactivity of those materials. These results show the difference in reactivity between both glasses. Ions release is slowed down by the organic matrix barrier but the 13-93B20 allow to remedy this effect compared to the 13-93 glass.

We developed gelatin/BAG hybrids using GPTMS as coupling agent, with a C_{factor} of 500, by a sol-gel method. The target mineral content (70/30 wt%) was guaranteed by careful control of the processing steps. The mineral phase dissolves when immersed in aqueous solution with kinetics depending on the glass composition. The mechanical properties varied as per the dissolution of the materials; however, the Young modulus remained close to value reported for cancellous bone. Both hybrids were found to precipitate hydroxy-carbonated apatite during immersion in SBF. The bioactivity seemed significantly higher when using the 13-93B20 glass. Therefore, preliminary cell experiments have been conducted to assess if the hybrids are biocompatible and thus, support the growth of pre-osteoblastic cells which is fundamental for a bone application.

3.3 MC3T3-E1 proliferation and morphology

MC3T3-E1 pre-osteoblastic cells were used to study their proliferation and morphology on the hybrids (Figure 10).

First, the number of MC3T3-E1 cells on the hybrids was studied for up to 14 days (Figure 10A). The hybrids were immersed 10 days in TRIS before cell culture to eliminate unreacted elements which can prevent cell survival [36]. The hybrids were placed in 48 well plates and the TCPS was used as a control. However, during their immersion in TRIS, they undergo a shrinking effect due the syneresis. Indeed, they go from a diameter of 11mm to 8mm in 10 days. Thus, to compare the proliferation on the control and the materials, the cell number was normalized to the area of the respective sample.

For each condition, the cells proliferate with time and reach a plateau indicating the stationary phase (Figure 9A). The glass 13-93 alone was already known to promote cell adhesion and proliferation as demonstrated by Fu et Al and Eqtesadi et Al [37,38]. At 14 days, the proliferation of MC3T3-E1 cells on G*/13-93B20 is significantly lower than on the control. This can be attributed to the release of boron from the borosilicate glass, known to decrease cell proliferation while promoting osteogenesis as observed in previous studies [13,39].

The morphology of the cells was observed at 24h, 7 days and 14 days on the control, G*/13-93 and G*/13-93B20 (Figure 10B). After 24h, it can be observed that the cells spread on both hybrids type with their characteristic polygonal morphology. There is no difference noted in the cytoskeleton of cells between the conditions. At 7 days and 14 days, multicellular layers are observed, covering the hybrids. These results show that the cells can spread, attach, and proliferate on the hybrids. Thus, the 13-93, the 13-93B20 and the GPTMS, do not present cytotoxic effects and do not prevent the proliferation and adhesion of MC3T3-E1 cells on the hybrids.

Preprints (www.preprints.org) | NOT PEER-REVIEWED | Posted: 28 January 2021 doi:10.20944/preprints202101.0594.v1

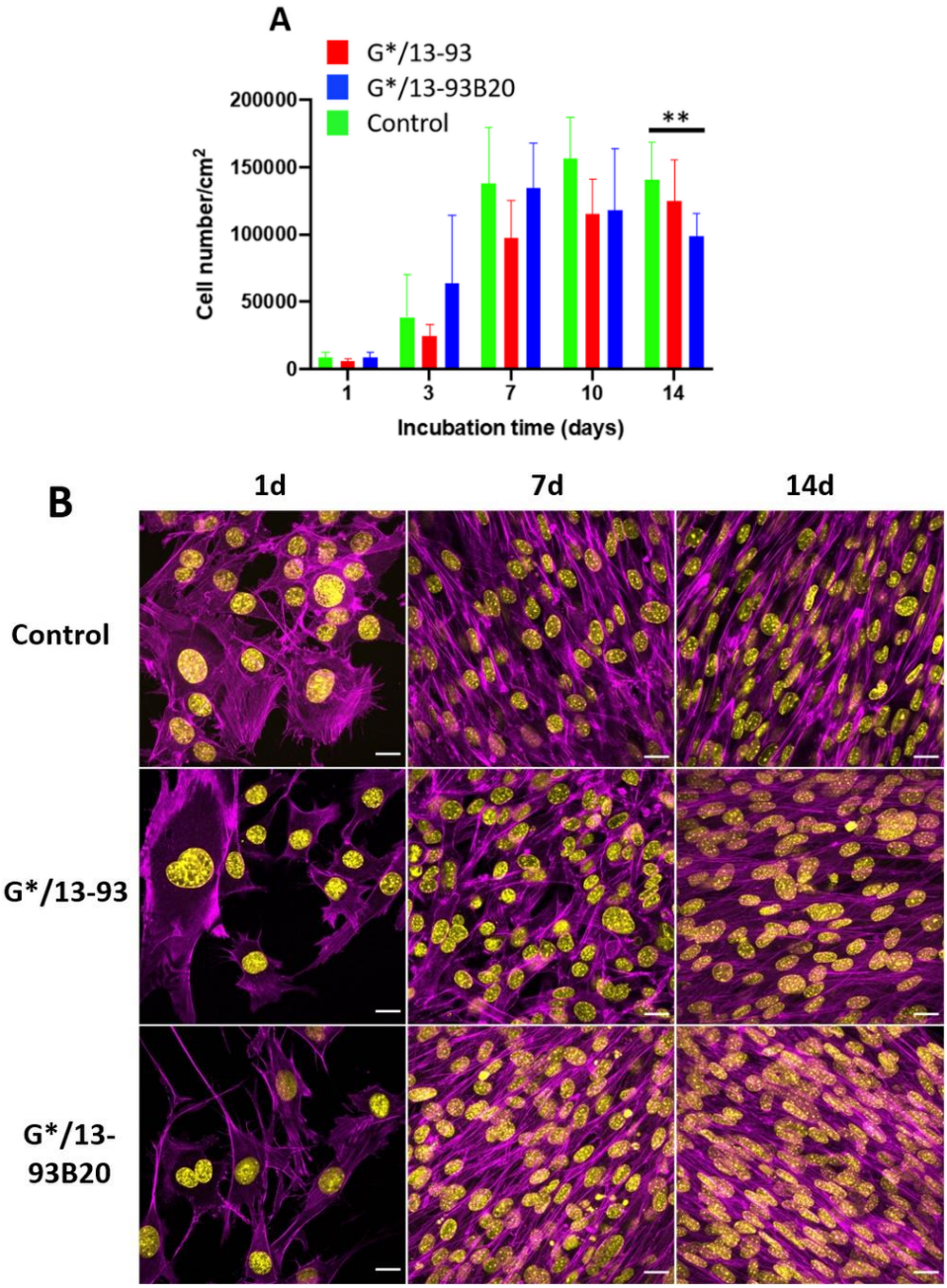

Figure 10: A) Proliferation of MC3T3-E1 cells cultured in αMEM complete medium on TCPS, G*/13-93 and G*/13-93B20 hybrids for 14 days, analyzed by CyQUANT Cell Proliferation Assay kit. The number of cells was normalized with the area of the materials surface (**p<0.01). B) Morphology of MC3T3-E1 cells in αMEM complete medium analyzed by Nuclei (DAPI - yellow) and Actin (Phalloidin - magenta) immunostaining after 1 day, 7 days and 14 days of culture. Scale bar 20μm.

4. Conclusion

Hybrids made of gelatin and BAG particles (silicate 13-93 and borosilicate 13-93B20) covalently linked with GPTMS were synthesized by the sol-gel method. The process of synthesis was optimized in order to obtain a content of organic/inorganic matter close to that was expected and to avoid particles sedimentation and aggregates. These hybrids were stable and self-supported at biological temperature in aqueous medium. When immersed in Simulated Body Fluid, their bioactivity was shown. Cells survival was demonstrated using MC3T3-E1 cells. The substitution of 20% of SiO_2 by B_2O_3 allowed to tailor the dissolution and bioactivity properties of the hybrids. Once stabilized, the hybrids exhibit mechanical properties which, combined with their ability to precipitate HA and their

biocompatible characteristic, make these materials good candidate for bone tissue engineering. Next studies will be done to investigate the osteo-stimulation of these materials.

Author Contributions: Conceptualization, A.H., M.B., J.M. and E.P.; methodology, R.A. and L.E.; validation, A.H., M.B., J.M. and E.P.; formal analysis, A.H., A.S. and M.L. (ICP analysis); investigation, A.H., M.B. and J.M.; resources, M.B., J.M. and E.P.; data curation, A.H., M.B. and J.M.; writing—original draft preparation, A.H.; writing—review and editing, M.B., J.M. and E.P.; supervision, M.B, J.M. and E.P.; project administration, M.B., E.P. and J.M.; funding acquisition, M.B. and E.P. All authors have read and agreed to the published version of the manuscript.

Funding: The authors thank ANR INEX Paris Seine Initiative for the doctoral fellowship.

Acknowledgments: The authors would like to thank the Science and Engineering Doctoral School of CY Cergy Paris Université for the financial support of the researcher mobility.

Conflicts of Interest: The authors declare no conflict of interest.

References

1. Schemitsch, E.H. Size Matters: Defining Critical in Bone Defect Size! *Journal of Orthopaedic Trauma* **2017**, *31*, S20–S22, doi:10.1097/BOT.0000000000000978.
2. Myon, L.; Ferri, J.; Chai, F.; Blanchemain, N.; Raoul, G. Ingénierie du tissu osseux oro-maxillofacial par combinaison de biomatériaux, cellules souches, thérapie génique. *Revue de Stomatologie et de Chirurgie Maxillo-faciale* **2011**, *112*, 201–211, doi:10.1016/j.stomax.2011.06.002.
3. Petrovic, V.; Zivkovic, P.; Petrovic, D.; Stefanovic, V. Craniofacial Bone Tissue Engineering. *Oral Surgery, Oral Medicine, Oral Pathology and Oral Radiology* **2012**, *114*, e1–e9, doi:10.1016/j.oooo.2012.02.030.
4. Kokubo, T. Apatite Formation on Surfaces of Ceramics, Metals and Polymers in Body Environment. *Acta Materialia* **1998**, *46*, 2519–2527, doi:10.1016/S1359-6454(98)80036-0.
5. Shimazaki, K.; Mooney, V. Comparative Study of Porous Hydroxyapatite and Tricalcium Phosphate as Bone Substitute. *Journal of Orthopaedic Research* **1985**, *3*, 301–310, doi:10.1002/jor.1100030306.
6. Ohura, K.; Bohner, M.; Hardouin, P.; Lemaître, J.; Pasquier, G.; Flautre, B. Resorption of, and Bone Formation from, New ?-Tricalcium Phosphate-Monocalcium Phosphate Cements: Anin Vivo Study. *Journal of Biomedical Materials Research* **1996**, *30*, 193–200, doi:10.1002/(SICI)1097-4636(199602)30:2<193::AID-JBM9>3.0.CO;2-M.
7. Schwach, G.; Vert, M. In Vitro and in Vivo Degradation of Lactic Acid-Based Interference Screws Used in Cruciate Ligament Reconstruction. *Int J Biol Macromol* **1999**, *25*, 283–291, doi:10.1016/s0141-8130(99)00043-4.
8. Hasegawa, S.; Ishii, S.; Tamura, J.; Furukawa, T.; Neo, M.; Matsusue, Y.; Shikinami, Y.; Okuno, M.; Nakamura, T. A 5–7 Year in Vivo Study of High-Strength Hydroxyapatite/Poly(l-Lactide) Composite Rods for the Internal Fixation of Bone Fractures. *Biomaterials* **2006**, *27*, 1327–1332, doi:10.1016/j.biomaterials.2005.09.003.
9. Verheyen, C.C.P.M.; de Wijn, J.R.; van Blitterswijk, C.A.; de Groot, K.; Rozing, P.M. Hydroxylapatite/Poly(L-Lactide) Composites: An Animal Study on Push-out Strengths and Interface Histology. *Journal of Biomedical Materials Research* **1993**, *27*, 433–444, doi:10.1002/jbm.820270404.
10. Ishikawa, K. Calcium Phosphate Cement. In *Advances in Calcium Phosphate Biomaterials*; Ben-Nissan, B., Ed.; Springer Berlin Heidelberg: Berlin, Heidelberg, 2014; pp. 199–227 ISBN 978-3-642-53980-0.
11. Hench, L.L. The Story of Bioglass®. *Journal of Materials Science: Materials in Medicine* **2006**, *17*, 967–978, doi:10.1007/s10856-006-0432-z.
12. Day, R.M.; Boccaccini, A.R.; Shurey, S.; Roether, J.A.; Forbes, A.; Hench, L.L.; Gabe, S.M. Assessment of Polyglycolic Acid Mesh and Bioactive Glass for Soft-Tissue Engineering Scaffolds. *Biomaterials* **2004**, *25*, 5857–5866, doi:10.1016/j.biomaterials.2004.01.043.

13. Houaoui, A.; Lyyra, I.; Agniel, R.; Pauthe, E.; Massera, J.; Boissière, M. Dissolution, Bioactivity and Osteogenic Properties of Composites Based on Polymer and Silicate or Borosilicate Bioactive Glass. *Materials Science and Engineering: C* **2020**, *107*, 110340, doi:10.1016/j.msec.2019.110340.
14. Mahony, O.; Tsigkou, O.; Ionescu, C.; Minelli, C.; Ling, L.; Hanly, R.; Smith, M.E.; Stevens, M.M.; Jones, J.R. Silica-Gelatin Hybrids with Tailorable Degradation and Mechanical Properties for Tissue Regeneration. *Advanced Functional Materials* **2010**, *20*, 3835–3845, doi:10.1002/adfm.201000838.
15. Novak, B.M. Hybrid Nanocomposite Materials - between Inorganic Glasses and Organic Polymers. *Adv. Mater.* **1993**, *5*, 422–433, doi:10.1002/adma.19930050603.
16. Nicole, L.; Boissière, C.; Grosso, D.; Quach, A.; Sanchez, C. Mesostructured Hybrid Organic–Inorganic Thin Films. *J. Mater. Chem.* **2005**, *15*, 3598, doi:10.1039/b506072a.
17. Liu, Y.-L.; Su, Y.-H.; Lai, J.-Y. In Situ Crosslinking of Chitosan and Formation of Chitosan–Silica Hybrid Membranes with Using γ-Glycidoxypropyltrimethoxysilane as a Crosslinking Agent. *Polymer* **2004**, *45*, 6831–6837, doi:10.1016/j.polymer.2004.08.006.
18. Mahony, O.; Yue, S.; Turdean-Ionescu, C.; Hanna, J.V.; Smith, M.E.; Lee, P.D.; Jones, J.R. Silica–Gelatin Hybrids for Tissue Regeneration: Inter-Relationships between the Process Variables. *Journal of Sol-Gel Science and Technology* **2014**, *69*, 288–298, doi:10.1007/s10971-013-3214-3.
19. Vueva, Y.; Connell, L.S.; Chayanun, S.; Wang, D.; McPhail, D.S.; Romer, F.; Hanna, J.V.; Jones, J.R. Silica/Alginate Hybrid Biomaterials and Assessment of Their Covalent Coupling. *Applied Materials Today* **2018**, *11*, 1–12, doi:10.1016/j.apmt.2017.12.011.
20. Maeda, H.; Kasuga, T.; Hench, L.L. Preparation of Poly(l-Lactic Acid)-Polysiloxane-Calcium Carbonate Hybrid Membranes for Guided Bone Regeneration. *Biomaterials* **2006**, *27*, 1216–1222, doi:10.1016/j.biomaterials.2005.08.010.
21. Vergnol, G.; Ginsac, N.; Rivory, P.; Meille, S.; Chenal, J.-M.; Balvay, S.; Chevalier, J.; Hartmann, D.J. *In Vitro* and *in Vivo* Evaluation of a Polylactic Acid-Bioactive Glass Composite for Bone Fixation Devices: POLYLACTIC ACID-BIOACTIVE GLASS COMPOSITE FOR BONE FIXATION DEVICES. *Journal of Biomedical Materials Research Part B: Applied Biomaterials* **2016**, *104*, 180–191, doi:10.1002/jbm.b.33364.
22. Brink, M. The Influence of Alkali and Alkaline Earths on the Working Range for Bioactive Glasses. *Journal of Biomedical Materials Research* **1997**, *36*, 109–117, doi:10.1002/(SICI)1097-4636(199707)36:1<109::AID-JBM13>3.0.CO;2-D.
23. Brown, R.F.; Rahaman, M.N.; Dwilewicz, A.B.; Huang, W.; Day, D.E.; Li, Y.; Bal, B.S. Effect of Borate Glass Composition on Its Conversion to Hydroxyapatite and on the Proliferation of MC3T3-E1 Cells. *Journal of Biomedical Materials Research Part A* **2009**, *88A*, 392–400, doi:10.1002/jbm.a.31679.
24. Ojansivu, M.; Mishra, A.; Vanhatupa, S.; Juntunen, M.; Larionova, A.; Massera, J.; Miettinen, S. The Effect of S53P4-Based Borosilicate Glasses and Glass Dissolution Products on the Osteogenic Commitment of Human Adipose Stem Cells. *PLoS ONE* **2018**, *13*, e0202740, doi:10.1371/journal.pone.0202740.
25. Maçon, A.L.B.; Kim, T.B.; Valliant, E.M.; Goetschius, K.; Brow, R.K.; Day, D.E.; Hoppe, A.; Boccaccini, A.R.; Kim, I.Y.; Ohtsuki, C.; et al. A Unified in Vitro Evaluation for Apatite-Forming Ability of Bioactive Glasses and Their Variants. *Journal of Materials Science: Materials in Medicine* **2015**, *26*, 115, doi:10.1007/s10856-015-5403-9.
26. Connell, L.S.; Gabrielli, L.; Mahony, O.; Russo, L.; Cipolla, L.; Jones, J.R. Functionalizing Natural Polymers with Alkoxysilane Coupling Agents: Reacting 3-Glycidoxypropyl Trimethoxysilane with Poly(γ-Glutamic Acid) and Gelatin. *Polymer Chemistry* **2017**, *8*, 1095–1103, doi:10.1039/C6PY01425A.
27. Griffith, L.G.; Naughton, G. Tissue Engineering--Current Challenges and Expanding Opportunities. *Science* **2002**, *295*, 7, doi:10.1126/science.1069210.
28. Hench, L.L. Bioceramics: From Concept to Clinic. *J American Ceramic Society* **1991**, *74*, 1487–1510, doi:10.1111/j.1151-2916.1991.tb07132.x.

29. Wu, D.; Isaksson, P.; Ferguson, S.J.; Persson, C. Young's Modulus of Trabecular Bone at the Tissue Level: A Review. *Acta Biomaterialia* **2018**, *78*, 1–12, doi:10.1016/j.actbio.2018.08.001.
30. Combes, C.; Cazalbou, S.; Rey, C. Apatite Biominerals. *Minerals* **2016**, *6*, doi:10.3390/min6020034.
31. Singh, R.; Tan, C.; Abd Shukor, M.; Sopyan, I.; Teng, W. The Influence of Ca/P Ratio on the Properties of Hydroxyapatite Bioceramics. *Proc SPIE* **2007**, *6423*, doi:10.1117/12.779890.
32. Huang, W.; Day, D.E.; Kittiratanapiboon, K.; Rahaman, M.N. Kinetics and Mechanisms of the Conversion of Silicate (45S5), Borate, and Borosilicate Glasses to Hydroxyapatite in Dilute Phosphate Solutions. *J Mater Sci: Mater Med* **2006**, *17*, 583–596, doi:10.1007/s10856-006-9220-z.
33. Stanislavov, A.S.; Sukhodub, L.F.; Sukhodub, L.B.; Kuznetsov, V.N.; Bychkov, K.L.; Kravchenko, M.I. Structural Features of Hydroxyapatite and Carbonated Apatite Formed under the Influence of Ultrasound and Microwave Radiation and Their Effect on the Bioactivity of the Nanomaterials. *Ultrasonics Sonochemistry* **2018**, *42*, 84–96, doi:10.1016/j.ultsonch.2017.11.011.
34. Baddiel, C.B.; Berry, E.E. Spectra Structure Correlations in Hydroxy and Fluorapatite. *Spectrochimica Acta* **1966**, *22*, 1407–1416, doi:10.1016/0371-1951(66)80133-9.
35. Berzina-Cimdina, L.; Borodajenko, N. Research of Calcium Phosphates Using Fourier Transform Infrared Spectroscopy. In *Infrared Spectroscopy - Materials Science, Engineering and Technology*; Theophanides, T., Ed.; InTech, 2012 ISBN 978-953-51-0537-4.
36. Maisani, M.; Pezzoli, D.; Chassande, O.; Mantovani, D. Cellularizing Hydrogel-Based Scaffolds to Repair Bone Tissue: How to Create a Physiologically Relevant Micro-Environment? *J Tissue Eng* **2017**, *8*, 1–26, doi:10.1177/2041731417712073.
37. Fu, Q.; Rahaman, M.N.; Bal, B.S.; Bonewald, L.F.; Kuroki, K.; Brown, R.F. Silicate, Borosilicate, and Borate Bioactive Glass Scaffolds with Controllable Degradation Rate for Bone Tissue Engineering Applications. II. In Vitro and in Vivo Biological Evaluation. *Journal of Biomedical Materials Research Part A* **2010**, *95A*, 172–179, doi:10.1002/jbm.a.32823.
38. Eqtesadi, S.; Motealleh, A.; Pajares, A.; Miranda, P. Effect of Milling Media on Processing and Performance of 13-93 Bioactive Glass Scaffolds Fabricated by Robocasting. *Ceramics International* **2015**, *41*, 1379–1389, doi:10.1016/j.ceramint.2014.09.071.
39. Ojansivu, M.; Mishra, A.; Vanhatupa, A.; Juntunen, M.; Larionova, A.; Massera, J.; Miettinen, S. The Effect of S53P4-Based Borosilicate Glasses and Glass Dissolution Products on the Osteogenic Commitment of Human Adipose Stem Cells. *PlosOne* **2018**, *13*, 1–20, doi:10.1371/journal.pone.0202740.